

Impact of processing conditions on wear of contact areas and performance of carbide tools with wear-resistant coatings

Vladimir P. Tabakov^{1,4}, Doctor of Sciences (Engineering), Professor

Oleg I. Morozov^{*1,2,5}, PhD (Engineering), Associate Professor

Renat U. Kamenov^{2,3,6}, PhD (Engineering)

¹Ulyanovsk State Technical University, Ulyanovsk (Russia)

²National Research University of Electronic Technology (MIET), Moscow (Russia)

³Togliatti State University, Togliatti (Russia)

*E-mail: oi.morozov@ulstu.ru

⁴ORCID: <https://orcid.org/0000-0002-2568-9401>

⁵ORCID: <https://orcid.org/0000-0001-8241-2591>

⁶ORCID: <https://orcid.org/0000-0001-9181-5704>

Received 28.08.2025

Revised 06.10.2025

Accepted 10.11.2025

Abstract: The use of wear-resistant coatings on tool contact areas is one of the most effective methods to enhance their durability and operational stability. However, when machining hard-to-cut materials, the effectiveness of such coatings decreases significantly, making it crucial to obtain new data on their failure mechanisms and develop improved coating compositions. This study investigates the influence of processing conditions, properties of the workpiece material, and the composition of wear-resistant coatings on the wear of contact areas and the performance of carbide tools. Single-layer TiN, TiZrN, and TiSiN coatings were examined, with an evaluation of their stress state and cyclic crack resistance. The contact areas of carbide inserts were studied using optical methods, and wear tests were conducted during turning with specialized equipment. It was demonstrated that both the type of workpiece material and the cutting conditions significantly affect the coating failure mode and tool life. The advantage of binary coatings, which possess enhanced mechanical properties and pronounced compressive residual stresses, was established. This contributes to increased cyclic crack resistance and improved fracture resistance. The obtained results can be used in developing technological processes for the finish machining of hard-to-cut materials, especially under minimum quantity lubrication (MQL) conditions or complete absence of cutting fluids.

Keywords: wear-resistant coating; carbide tool; crack resistance; wear; performance; hard-to-cut materials

Acknowledgements: The study was funded by the Russian Science Foundation (grant No. 22-19-00298-P), <https://rscf.ru/project/22-19-00298/>.

For citation: Tabakov V.P., Morozov O.I., Kamenov R.U. Impact of processing conditions on wear of contact areas and performance of carbide tools with wear-resistant coatings. *Frontier Materials & Technologies*, 2025, no. 4, pp. 89–101. DOI: <https://doi.org/10.18323/2782-4039-2025-4-74-8>.

INTRODUCTION

The application of wear-resistant coatings on tool contact areas has proven to be one of the most effective techniques for enhancing durability and operational stability. Operational experience has shown that applying single-element coatings when machining structural materials – regardless of whether continuous or intermittent cutting is used – allows increasing tool life by 1.75 to 4 times, depending on the coating composition and processing conditions. For example, applying TiAlN coatings when turning SCh18 workpieces increases the service life of VK8 inserts by 3.3 times [1]. Similar results for TiAlN coatings are presented in reference [2]. Recent studies on multilayer systems based on TiAlN/TiSiN/ZrN and TiAlSiN/AlCrN report increased hardness, oxidation resistance, and wear resistance due to nanolamination and optimisation of layer architecture [3; 4].

The improvement of mechanical properties in coatings can be achieved by introducing nickel and copper. Studies

[5; 6] have found that the application of TiAlN-Cu and TiAlN-Ni coatings increases the tool life of carbide inserts by 3.1 and 1.7 times, respectively, during turning of 09G2S steel workpieces. Similar results were obtained when milling EP302-Sh steel workpieces. However, the substrate also significantly influences the results: increasing the TiC proportion and introducing TaC into WC-Co improves the adhesion and wear resistance of TiAlN films [7]. Furthermore, the thickness of the TiAlN coating affects surface roughness, residual stresses, and fatigue durability when turning Inconel 718 – an optimal coating thickness exists for specific cutting conditions [8].

Ternary nitride coatings demonstrate even higher efficiency; their application additionally increases the tool life of carbide tools by 1.3 to 2.27 times compared to binary coatings. Ternary and quaternary nitride coatings of the Ti–Al–Cr system with Si and Y additions, such as (TiAlCr)N, (AlTiCr)N, and (TiAlCrSiY)N, are characterised by retained hardness at elevated temperatures, improved thermal

stability, and high oxidation resistance due to the formation of protective Al_2O_3 and Cr_2O_3 oxide films on the working surface. The nanolaminated architecture of such systems increases the number of interphase boundaries, which improves stress distribution and reduces the tendency for delamination. As a result, the development of crater wear is slowed, and coating behaviour is stabilised when milling quenched and stainless steels, as well as nickel-based superalloys [9]. For AlCrN coatings, it has been experimentally demonstrated that when milling quenched SKD11 steel, switching to environmentally friendly cooling and lubrication strategies, such as MQL, cryogenic cooling, and their hybrid variants, reduces wear intensity and improves surface quality compared to dry cutting [10]. For TiAlVN, when milling Inconel 718, the dominant mechanisms of coating and cutting edge failure have been clarified, including adhesive and abrasive wear and localised delamination, with pronounced sensitivity to cutting conditions confirmed experimentally [11].

High efficiency of cutting tools is ensured by the application of multilayer coatings. For modern multilayer nanostructured systems (e.g., TiAlN/TiSiN/ZrN), improvements in tribological characteristics and suppression of crack propagation and delamination are noted, which is attributed to barrier interfaces and stress distribution [3]. Meanwhile, the multilayer TiAlSiN/AlCrN combination demonstrates increased resistance to high-temperature oxidation and better wear resistance compared to monolayer coatings [4].

In recent years, single- and multilayer coatings with nanostructured layers have been actively studied [12–14]. Research has shown that for machining heat-resistant alloys (e.g., Inconel 718), optimisation of coating composition (Al, Si, Cr, V) and architecture (nanolamination, HiP-IMS) reduces adhesive-abrasive wear, stabilises crater formation, and enhances tool life [15–17]. Specifically, when milling Hastelloy C276 and quenched SKD11 steel, environmentally friendly cooling strategies (MQL, cryogenic, hybrid methods) applied to tools with TiSiN/TiAlN/AlCrN coatings improve surface quality and slow wear compared to dry cutting [10; 17]. For materials prone to sticking, TiAlN/DLC hybrid systems demonstrate the reduction in adhesive wear and stabilisation of the cutting processes [18].

Significantly lower effectiveness of wear-resistant coatings is observed when machining stainless steel workpieces. The cutting process when treating these steels is accompanied by high levels of mechanical loads and intense heat generation. Under such conditions, high adhesive strength, crack resistance, and oxidation stability of the coatings are critical, as is the correct selection of cooling strategies [16]. Nevertheless, even when working with nickel-based superalloys and austenitic steels, proper adjustment of the coating composition and architecture can significantly reduce wear intensity [11; 15], while the selection of an appropriate cooling strategy further reduces wear and improves surface quality [10].

The aforementioned issues necessitate the search for new, more effective compositions and designs of wear-resistant coatings. This requires data on the influence of

processing conditions on the failure mechanism of coatings on the contact areas of cutting tools.

The aim of the study is to establish the relationships between coating composition and the wear of contact areas of carbide tools, as well as their performance during turning of workpieces made of materials with different machinability characteristics.

METHODS

Research objects and materials

As part of this work, single-layer wear-resistant TiN, TiZrN, and TiSiN coatings were investigated. The coatings were deposited onto carbide MS318 and VK6 inserts using a Bulat-3T system (Russia). During the formation of TiN, three titanium cathodes were used: two titanium cathodes were employed to produce TiZrN, and one composite cathode with a zirconium insert. The deposition of TiSiN was carried out using two cathodes made of a titanium-silicon alloy and an additional titanium cathode.

Determination of mechanical properties of coatings

The mechanical properties of the coatings were determined according to the methodologies described in [19]. Microhardness and elastic modulus were measured using a Mitutoyo NH-125 microhardness tester (Japan). For microhardness measurements, a Vickers pyramid was used under a 1 N load, while a Knoop pyramid was employed under a 2.6 N load for the elastic modulus determination, which was calculated using the formula

$$E = \frac{HV - \alpha}{\frac{b_1}{d_1} - \frac{b}{d}},$$

where HV is the Knoop microhardness, GPa;

α is a dimensionless coefficient ($\alpha=0.45$);

b_1 , b are the short diagonals of the Knoop pyramid impression on the lead reference sample and the test sample, respectively;

d_1 , d are the long diagonals of the impression.

Knoop microhardness was determined as

$$HV = \frac{12.89 \cdot P}{d^2}.$$

Calculation of crack resistance parameters

The critical stress intensity factor K_I was calculated using the formula:

$$K_I = \frac{E}{8K(1-\nu^2)} \cdot \sqrt{\frac{a}{2\pi(1-\nu^2)}},$$

where K is a coefficient ($K=0.107$);

ν is the Poisson's ratio ($\nu=0.3$);

a is the crystal lattice parameter, m.

The fracture toughness K_{IC} was determined as

$$K_{IC} = 0.035\sigma_y \sqrt{C} \left(\frac{E}{\sigma_y} \right)^{0.4} \left(\frac{C}{c} - 1 \right)^{-\frac{1}{2}},$$

where σ_y is the yield strength, GPa;
 c is the indentation size, m;
 C is the length of the Palmqvist crack, m.

Evaluation of the stress state of coatings

The stress state parameters and cyclic crack resistance indicators were calculated using approaches described in [20].

The stress state of the coatings was evaluated based on the magnitude of the total stresses arising during cutting, which were determined from the expression:

$$\sigma_{\Sigma} = \sigma + \sigma_{creep},$$

where $\sigma = \sigma_1 + \sigma_{therm} + \sigma_{res} + \sigma_{creep}$;
 σ_1 is stresses caused by mechanical and thermal loads during cutting;
 σ_{therm} is thermal stresses caused by the difference in the coefficients of thermal expansion of the coating and the substrate;
 σ_{res} is residual stresses in the coating;
 σ_{creep} is stresses induced by creep of the tool wedge material.

The σ_1 component generated during the direct interaction between the tool and a workpiece was calculated from the condition of strain compatibility between the coating and the substrate, taking into account the acting stresses σ_x . The calculation was performed using the dependence:

$$\sigma_1 = \frac{E}{E_0} \sigma_x,$$

where E and E_0 are the elastic moduli of the coating and the tool substrate, respectively.

The thermal stress component σ_{therm} , associated with the difference in the coefficients of linear expansion between the substrate and the coating, was determined by the expression

$$\sigma_{therm} = (\alpha_0 - \alpha_c) E \cdot \frac{\Delta T}{(1 - \nu)},$$

where α_0 and α_c are the coefficients of thermal expansion of the substrate and coating materials, respectively;
 ΔT is the difference between the contact temperature on the rake face of the tool and ambient conditions;
 ν is the Poisson's ratio.

Residual stresses σ_{res} were determined using a DRON-3M X-ray diffractometer. The stresses σ_x and temperature on the rake face, required for calculating σ_1 and σ_{therm} , were determined from temperature fields and stress fields in the tool wedge. These fields were obtained using the ANSYS software package and experimental data on the contact characteristics of the cutting process.

The contribution of the creep of the cutting wedge material to the overall stress state was evaluated using the dependence

$$\sigma_{creep} = EA\sigma_x^k t^{\frac{1}{3}},$$

where A and k are coefficients dependent on the wedge material properties and temperature level;
 t is the tool operating time.

Determination of cyclic crack resistance

Of particular interest was the cyclic crack resistance of the coating t_c , which reflects the time until crack initiation and is calculated as the sum of two terms:

$$t_c = t_{c1} + t_{c2},$$

where t_{c1} is the period of transition of compressive stresses to tensile stresses;

t_{c2} is the time for a germ crack to develop to a critical.

For the first component, the expression was used:

$$t_c = \left(\frac{\sigma_1 + \sigma_y + \sigma_0 + \Delta\sigma}{EA\sigma_x^k} \right)^3,$$

where $\Delta\sigma$ is the stress amplitude in the cycle.

The second t_{c2} component was determined numerically using an integral relation

$$\int_{l_0}^h \frac{dl}{c^4 l^2} = \int_0^{t_{c2}} \frac{1,09\pi^2}{2K_{IC}^2 \sigma_y^2 t_1} \cdot (\sigma_{max}^4 - \sigma_{min}^4) dt,$$

where C is the crack shape factor;

l_0 is the size of the germ crack;

h is the coating thickness;

K_{IC} is the fracture toughness of the coating material;

σ_y is the yield strength of the coating material;

t_1 is the chip formation element time (determined according to the methodology in [19]);

σ_{min} and σ_{max} are the extreme stresses per cycle.

Methods of experimental research

To study the contact areas of carbide inserts with wear-resistant coatings, a JSM-35CF scanning electron microscope (Japan) was used. Wear tests were conducted under turning conditions using workpieces made of 30HGSA and 12H18N10T steels, as well as SCh30 cast iron and VT22 titanium alloy. Tool performance was evaluated based on tool life determined when flank wear reached 0.4 mm during turning of workpieces made of 30HGSA and 12H18N10T steels.

For each coating variant, tests were conducted at least three times. The values presented in the tables are averages; statistical processing of the results included calculation of the standard deviation. The scatter of the obtained data did not exceed 5–7 % of the average values, confirming the reproducibility of the results.

RESULTS

Phase composition and physical and mechanical properties of coatings

Analysis of the phase composition of the studied wear-resistant coatings revealed that they all exhibit a single-phase structure with the presence of the TiN phase. As an illustration, Fig. 1 shows a fragment of the diffraction pattern for the TiZrN coating.

Data in Table 1 demonstrate that the binary coatings possess higher microhardness and elastic modulus, which results in their improved crack resistance, reflected in high fracture toughness values.

Coating behaviour during machining of 30HGSA steel

Analysis of the contact areas on carbide inserts with wear-resistant coatings revealed that when turning workpieces of 30HGSA steel under a range of cutting conditions (cutting speed $V=100\text{--}180$ m/min, feed rate $s=0.15\text{--}0.3$ mm/rev, and depth of cut $t=0.5$ mm), and with flank wear up to $h_f=0.4$ mm, the coatings remain on the tool's rake face. The presence of the coating significantly influences the wear mechanism: the characteristic crater wear on the rake face, typical of uncoated inserts, is absent. Instead, a change in the cutting wedge geometry is observed bulging occurs on both the rake and flank surfaces, with this phenomenon being most pronounced at high cutting speeds.

On the oblique section shown in Fig. 2 a, the deformation of the cutting edge of the carbide insert, the bulging of the carbide substrate material and the fully preserved coating on the rake face are clearly visible. At the same time, flank wear begins with the wear of the bulged portion of the carbide base material, and the wear land is not contiguous with the cutting edge (Fig. 2 b). Subsequently, as the carbide insert continues to operate, a classical flank wear land forms. The deformation of the cutting wedge of the carbide inserts is accompanied by the descent of its tip, the magnitude of which depends on the coating composition (Fig. 3).

The study showed that the magnitude of the cutting wedge tip descent h_γ increases with increasing cutting speeds and feed rates. Furthermore, for carbide inserts with multicomponent coatings, the value of h_γ is smaller compared to those with a TiN coating. As can be seen from Fig. 3, for carbide inserts with a TiN coating, the wedge tip descent magnitude reached $12\ \mu\text{m}$ after 14 min of operation, whereas for inserts with TiZrN and TiSiN coatings, the value of h_γ reached $12\ \mu\text{m}$ only after 28 and 31 min of operation, respectively. Therefore, multicomponent coatings provide greater shape stability of the wedge in carbide inserts compared to single-component coatings.

Crack formation and coating wear

Studies of the contact areas on coated carbide inserts have found that when machining 30HGSA steel workpieces, the coatings are completely preserved on the rake face. During the process of cutting carbide inserts, cracks form in the coating (Fig. 4). Their initiation is associated with the action of equivalent stresses on the rake face, as well as with fatigue processes and adhesion occurring during chip movement along the rake face.

As the tool operates, the cracks on the rake face increase in size and are observed to propagate into the carbide substrate. The growth of the cracks is accompanied by brittle fracture of the coating along the crack length, which is clearly visible in Fig. 4, and the detachment of individual coating fragments. Despite this, the coating remains on the rake face of the carbide inserts, continuing to perform its protective functions (Fig. 4).

The coating composition does not significantly affect the mechanism of crack initiation and growth; however, it directly determines the duration for which carbide inserts remain operational before the first damage occurs. Multicomponent coatings are characterised by a shift in the initiation toward higher cutting speeds compared to single-layer TiN. For instance, on MS318 inserts with TiN coating, cracks were observed at speeds as low as 100 m/min ($s=0.15$ mm/rev, $t=0.5$ mm) across the entire contact area on the rake face. In contrast, for TiZrN and TiSiN coatings,

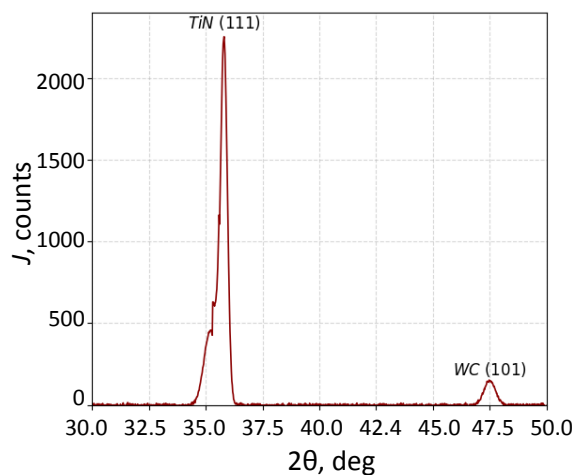
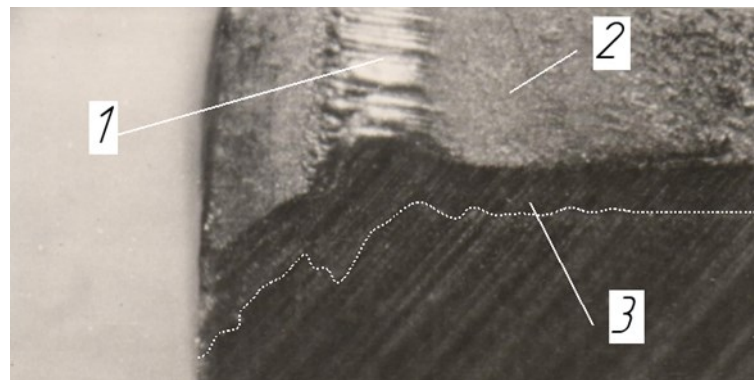


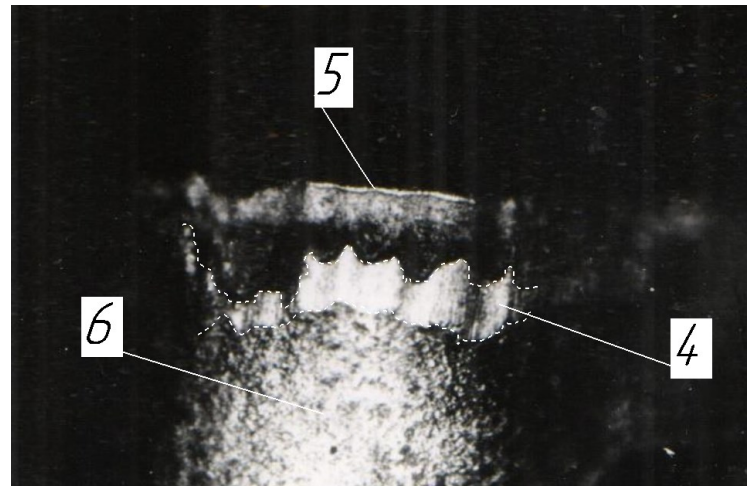
Fig. 1. Fragment of the diffractogram of the TiZrN coating
Рис. 1. Фрагмент дифрактограммы покрытия TiZrN

Table 1. Mechanical properties of wear-resistant coatings
Таблица 1. Механические свойства износостойких покрытий

Coating	Knoop microhardness HV , GPa	Elastic modulus E , GPa	Critical stress intensity factor K_{Ic} , $MPa \cdot m^{1/2}$	Fracture toughness K_{Ic} , $MPa \cdot m^{1/2}$
TiN	31.45	307	3.39	12.29
TiZrN	41.91	379	4.22	14.44
TiSiN	37.39	350	3.88	14.46



a



b

Fig. 2. Rake face bulging (*a*) and wear of the bulged carbide base material on the flank face (*b*) during processing of a 30HGSA steel workpiece using VK6 carbide inserts at $V=200$ m/min, $s=0.45$ mm/rev, $t=1.0$ mm (operating time 24 min).
 1 – bulging; 2 – rake face; 3 – coating; 4 – wear on the bulged part of the carbide base; 5 – main cutting edge; 6 – main flank face

Рис. 2. Выпучивание по передней поверхности (*a*) и износ выпученного материала твердосплавной основы по задней поверхности (*b*) при обработке заготовки из стали 30ХГСА твердосплавными пластинами ВК6 при $V=200$ м/мин, $s=0,45$ мм/об, $t=1,0$ мм (время работы 24 мин).
 1 – выпучивание; 2 – передняя поверхность; 3 – покрытие; 4 – износ по выпученной части твердосплавной основы; 5 – главная режущая кромка; 6 – главная задняя поверхность

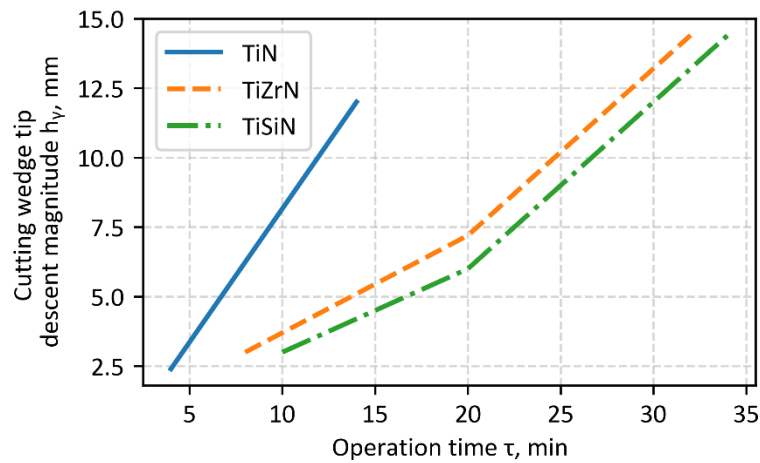


Fig. 3. Effect of the operation time of MS318 carbide inserts on the cutting wedge tip descent magnitude (h_γ) when processing 30HGSA steel workpieces at $V=150$ m/min, $s=0.3$ mm/rev, $t=0.75$ mm (operation time is 5 min)
Рис. 3. Влияние времени работы твердосплавных пластин MC318 при обработке заготовок из стали 30ХГСА на величину опускания вершины режущего клина h_γ при $V=150$ м/мин, $s=0,3$ мм/об, $t=0,75$ мм (время работы 5 мин)

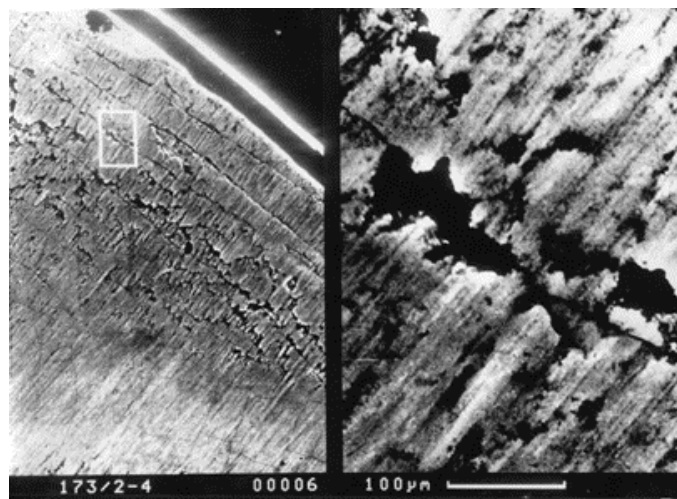


Fig. 4. Contact area on the rake face of MS318 carbide inserts (secondary electron image) with a TiN coating during turning of a 30HGSA steel workpiece at $V=100$ m/min, $s=0.3$ mm/rev, $t=0.5$ mm
Рис. 4. Контактная площадка на передней поверхности твердосплавных пластин MC318 (изображение во вторичных электронах) с покрытием TiN при токарной обработке заготовки из стали 30ХГСА при $V=100$ м/мин, $s=0,3$ мм/об, $t=0,5$ мм

the first defects appeared only at speeds above 170 m/min. Moreover, the failure process developed more rapidly in TiZrN. For example, during machining at 180 m/min, crack formation in the TiSiN coating was detected after approximately 20 min of operation, whereas for TiZrN, it occurred within just 10–12 min.

When machining SCh30 cast iron, VT22 alloy, and 12H18N10T stainless steel, the wear pattern differed from that observed during turning of 30HGSA steel. Observations using characteristic radiation and backscattered electrons revealed that coating degradation begins within

the first minutes of cutting. Nevertheless, a significant portion of the coating persists on the contact surface. With increased machining time, the damaged area expands, but the presence of isolated coating “islands” within the contact zone and along the cutting edge slows flank face wear. Over time, a crater wear forms on this surface. The presence of the coating substantially reduces its progression rate, limiting both depth and width growth.

For example, when turning 12H18N10T stainless steel (Fig. 5), once the flank wear land reached 0.4 mm, the crater wear with depth and width of approximately

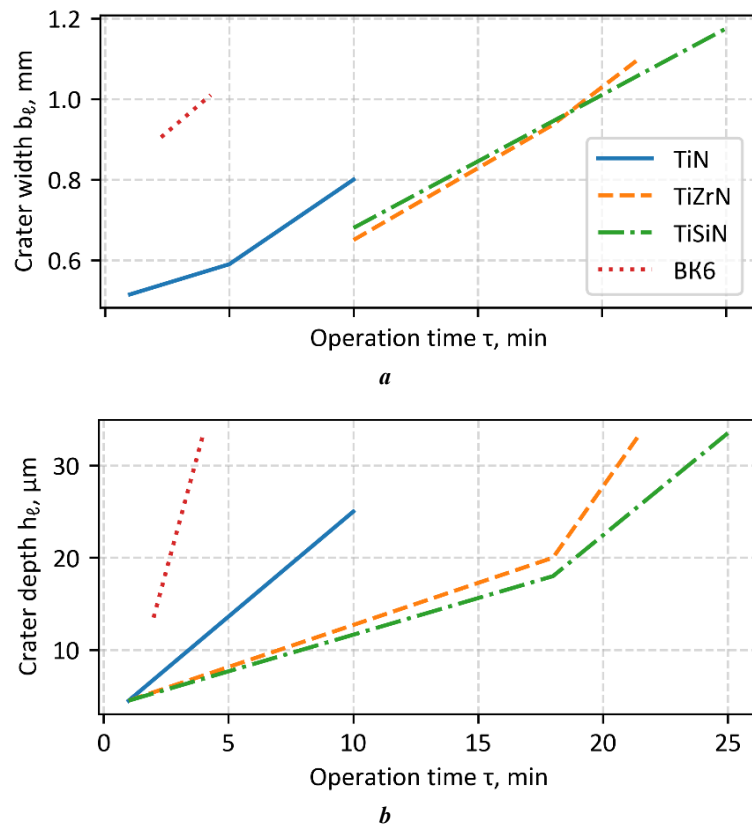


Fig. 5. Effect of coatings on rake face wear parameters of VK8 carbide inserts when machining 12H18N10T steel ($V=100$ m/min, $s=0.3$ mm/rev, $t=0.75$ mm):
a – crater wear width (b); **b** – crater wear depth (h)

Рис. 5. Влияние покрытий на параметры износа по передней поверхности твердосплавных пластин BK8 при обработке стали 12Х18Н10Т ($V=100$ м/мин, $s=0,3$ мм/об, $t=0,75$ мм):
a – ширина лунки износа (b); **b** – глубина лунки износа (h)

35 μm and 1.04 mm respectively was developed after merely 5 min of operation with uncoated inserts. When applying TiN coating, similar depth (25 μm) was recorded only after 10 min, with corresponding width of 0.8 mm. An even more pronounced effect was observed for TiZrN and TiSiN coatings: the 25- μm depth threshold was reached only after 20 and 23 min of machining respectively, with crater widths of 0.9 mm for TiZrN and 1.1 mm for TiSiN (Fig. 5).

It is important to note that compared to uncoated inserts, the protective coatings more effectively inhibit crater propagation toward the cutting edge than in the chip flow direction. This wear distribution pattern positively influences the overall tool performance. Furthermore, binary coatings exhibit slower degradation rates due to their enhanced mechanical properties.

Stress state and crack resistance of coatings

The structural parameters, mechanical properties, and stress state indices used in the calculations for various coatings are presented in Table 2.

The results of the stress state and cyclic crack resistance calculations are further summarised in Tables 3 and 4 and visualised in Fig. 6 and 7. For example, coated inserts tested during machining of 30HGSA steel under the cutting conditions of $V=180$ m/min, $s=0.15$ mm/rev, and $t=0.5$ mm were considered.

Table 3 demonstrates that the total stresses σ are compressive, and for binary coatings, they are higher compared

to the TiN coating: approximately 24 % higher for the TiZrN coating and 15 % higher for the TiSiN coating.

The change in creep stresses over time is shown in Fig. 6. The lowest values of this parameter were recorded for the TiSiN coating. For TiZrN, the σ_c level was approximately 5 % higher than that of TiN. After 5 min of tool operation, creep stresses in the TiSiN layer were 24 % lower, while for the TiZrN coating, they exceeded TiN values by 6 %. Meanwhile, taking into account creep stresses after 5 min of tool operation, the total stresses σ_x in the TiSiN coating remained compressive (–11 MPa), while in TiZrN and TiN coatings, they transformed into tensile stresses. Furthermore, higher stress values were observed for TiN coatings (1044 MPa for TiN and 751 MPa for TiZrN) (Table 3).

During tool service, the nature of total stresses σ_x changed: they gradually transformed from compressive to tensile (Fig. 7). This transition occurs after more than 5 min of tool operation for TiSiN coatings, while for TiZrN and TiN coatings it occurs after more than 2 and 1 min of operation, respectively. The obtained data indicate that TiSiN coatings are more resistant to crack formation.

The cyclic crack resistance of coatings is presented in Table 4. It is evident that components of cyclic crack resistance for binary coatings are significantly higher compared to TiN coating, with the maximum values characteristic

Table 2. Structural parameters, mechanical properties, and stress state indices of coatings
Таблица 2. Структурные параметры, механические характеристики и показатели напряженного состояния покрытий

Coating	Germ crack size l_0 , nm	Coating material yield strength σ_y , GPa	Fracture toughness K_{IC} , $\text{MPa}\cdot\text{m}^{1/2}$	Chip element formation time t_f , s	Stress oscillation amplitude per cycle $\Delta\sigma$, MPa
TiN	0.5990	9.53	12.29	$5.60\cdot 10^{-5}$	241
TiZrN	0.6072	12.38	14.44	$7.11\cdot 10^{-5}$	174
TiSiN	0.6018	11.17	14.46	$6.38\cdot 10^{-5}$	202

Table 3. Stress state parameters of coatings
Таблица 3. Параметры напряженного состояния покрытий

Coating	σ_1 , MPa	σ_r , MPa	σ_t , MPa	σ , MPa	σ_{creep}^* , MPa	σ_{Σ}^* , MPa
TiN	546	-775	-1827	-2056	3100	1044
TiZrN	613	-1256	-1906	-2549	3300	751
TiSiN	565	-1069	-1857	-2361	2350	-11

Note. σ_1 is load-induced stresses; σ_r is residual stresses in coating; σ_t is thermal stresses; σ is calculated stress component; σ_{creep} is stresses due to tool wedge material creep; σ_{Σ} is total stresses.

* After 5 min of operation.

Примечание. σ_1 – напряжения, обусловленные нагрузками; σ_r – остаточные напряжения в покрытии; σ_t – термические напряжения; σ – расчетная компонента напряжений; σ_{creep} – напряжения, вызванные ползучестью материала режущего клина инструмента; σ_{Σ} – суммарные напряжения.

* После 5 мин работы.

Table 4. Cyclic crack resistance of coatings
Таблица 4. Циклическая трещиностойкость покрытий

Coating	Tool operation time until compressive-to-tensile stress transition t_{c1} , min	Time until coating failure initiation t_{c2} , min	Cyclic crack resistance magnitude t_c , min
TiN	1.4	6.25	7.65
TiZrN	2.37	11.43	13.8
TiSiN	5.43	18.75	24.18

of TiSiN coating. Specifically, the t_{c1} component characterising tool operation time until compressive stress transition to tensile reaches maximum magnitude for TiSiN coating, being 2.3 times greater than that of the TiZrN coating and 3.9 times greater than that of the TiN coating. The time until coating failure initiation t_{c2} and the cyclic crack resistance magnitude also achieve maximum values, surpassing TiZrN by 1.6 and 1.75 times, respectively, and exceeding TiN by 3 and 3.2 times, respectively.

Tool life of carbide inserts

Tool life tests of carbide inserts during turning of 30HGSA and 12H18N10T steel workpieces confirmed the superior effectiveness of binary coatings compared to TiN (Fig. 8). The TiSiN coating demonstrated the highest performance. TiSiN coating application provides the greatest improvement in tool life for carbide inserts regardless of the workpiece material grade. When machining 30HGSA steel workpieces, the tool life of TiSiN-coated carbide

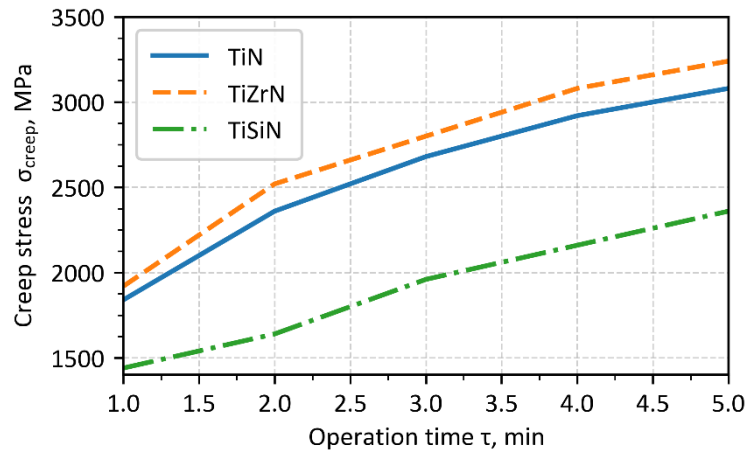


Fig. 6. Dynamics of creep stress (σ_{creep}) evolution in coatings within the chip–rake face contact zone depending on tool operation time (t)
Рис. 6. Динамика изменения напряжений ползучести (σ_{creep}) в покрытиях в зоне контакта стружки с передней поверхностью в зависимости от времени работы инструмента (t)

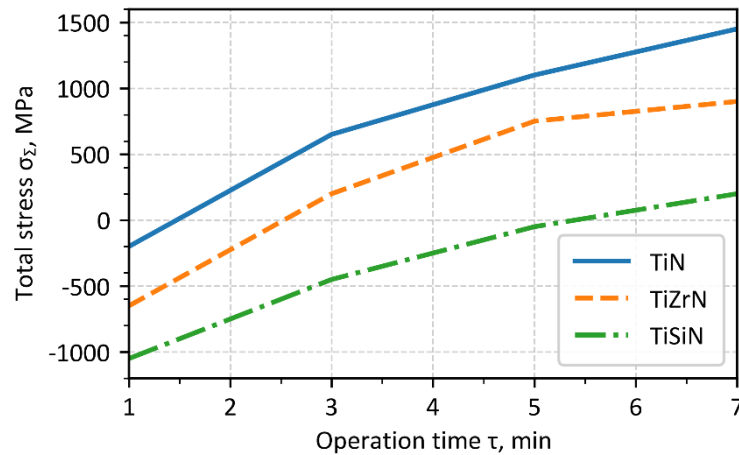


Fig. 7. Change in total stresses (σ_{Σ}) in coatings at the center of chip–rake face contact zone over time (t)
Рис. 7. Изменение суммарных напряжений (σ_{Σ}) в покрытиях в середине контакта стружки с передней поверхностью во времени (t)

inserts was 1.2–1.6 times longer compared to TiZrN coating and 2.6–3.5 times longer compared to TiN. For 12H18N10T steel machining, the tool life values were 1.25–1.3 times and 1.6–1.8 times respectively, depending on cutting speed (Fig. 8).

DISCUSSION

Analysis of the contact areas on carbide inserts reveals that coating failure exhibits brittle characteristics and significantly depends on the workpiece material. When machining 30HGSA alloy steel workpieces, the coatings on the rake face do not fracture completely but develop cracks whose propagation dynamics are determined by the coating composition. During machining of SCh30 cast iron work-

pieces, abrasive action of the material leads to coating failure within the first minutes of cutting. Similar coating degradation occurs when cutting 12H18N10T steel and VT22 titanium alloy workpieces. Furthermore, the development of crater wear on the rake face also depends on coating composition. The TiSiN coating most effectively restrains both coating failure and rake face wear, which can be attributed to its superior mechanical properties.

Studies of coating stress states and their cyclic crack resistance demonstrated that binary coatings provide superior resistance to crack initiation and propagation compared to TiN coating. These coatings are characterised by higher overall compressive stresses generated during cutting, which inhibit crack development processes. Due to their enhanced mechanical properties, the stresses caused

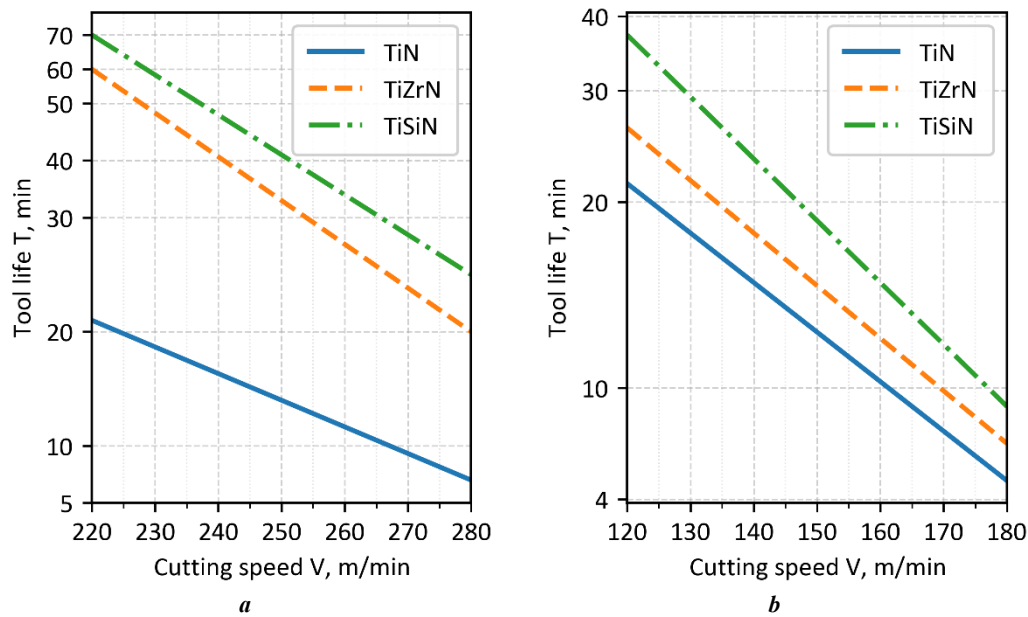


Fig. 8. Effect of cutting speed V on the tool life T of coated carbide inserts when machining steel workpieces: **a** – 30HGSA steel with MS318 insert; **b** – 12H18N10T steel with VK6 insert; $s=0.15$ mm/rev; $t=0.5$ mm

Рис. 8. Влияние скорости резания V на период стойкости T твердосплавных пластин с покрытиями при обработке заготовок из сталей: **a** – 30ХГСА, пластина марки МС318; **b** – 12Х18Н10Т, пластина марки ВК6; $s=0,15$ мм/об; $t=0,5$ мм

by cutting wedge creep are lower in binary coatings than in TiN coatings. The minimum creep stress values occur in TiSiN coating, resulting in the formation of the highest resultant stresses. Consequently, the duration of their transition from compressive to tensile state exceeds that of TiZrN and TiN coatings. This leads to higher cyclic crack resistance of TiSiN coating compared to TiZrN and especially TiN coating. The obtained data on evaluation of stress state and cyclic crack resistance are in good agreement with the results of studies on coating failure and the effect of coatings on rake face wear. The TiSiN coating, which has the highest cyclic crack resistance, significantly inhibited rake face wear of carbide inserts when machining workpieces made of SCh30 cast iron, 12H18N10T steel, and VT22 titanium alloy. It also facilitated a longer service life of the inserts before crack formation when machining workpieces made of 30HGSA steel compared to TiZrN and TiN coatings.

The conducted wear resistance studies confirmed the high efficiency of binary coatings compared to TiN, with the TiSiN coating providing the greatest increase in tool life of carbide inserts. The enhanced performance of TiZrN and TiSiN coatings is attributed to the introduction of additional elements (Zr, Si), which form a more ductile and crack-resistant structure capable of reducing the friction coefficient in the contact zone, particularly when machining titanium alloys. This enables significant retardation of wear development on surfaces operating primarily under frictional conditions, such as the rake and flank faces during turning operations.

The research findings suggest that these coatings could be effectively used in the manufacture of working surfaces of the tool for surface plastic deformation processes where tool durability under intensive friction conditions is critical. This is particularly important in the context of the transition

from traditional cutting fluid applications to environmentally friendly regimes, including machining with minimum quantity lubrication (MQL) and completely dry cutting.

CONCLUSIONS

1. It has been found that the properties of the workpiece significantly influence the failure of coatings during cutting. When machining 30HGSA steel workpieces, the coatings are completely preserved at the rake face, preventing crater formation. When machining workpieces made of SCh30 cast iron, 12H18N10T stainless steel, and VT22 titanium alloy, the coatings deteriorate within the first minutes of carbide insert operation, followed by crater wear development on the rake face.

2. It has been determined that TiSiN coating provides the greatest resistance to crack initiation and propagation, characterised by the highest total compressive stresses that suppress crack formation and development, along with superior cyclic crack resistance compared to TiZrN and TiN coatings.

3. It has been demonstrated that TiSiN coating provides the greatest increase in the service life of carbide inserts. Compared to TiZrN and TiN coatings, the service life of TiSiN-coated carbide inserts is 1.2–3.5 times longer, depending on coating composition, workpiece material, and processing parameters.

REFERENCES

- Zhou Jun, Liao Hengcheng, Chen Hongmei, Feng Di, Zhu Weijun. Realizing strength-ductility combination of $Fe_{3.5}Ni_{3.5}Cr_2MnAl_{0.7}$ high-entropy alloy via coherent dual-phase structure. *Vacuum*, 2023, vol. 215, article number 112297. DOI: [10.1016/j.vacuum.2023.112297](https://doi.org/10.1016/j.vacuum.2023.112297).

2. Kabaldin Y.G., Seryi S.V., Murav'ev S.N., Prosolovich A.A., Simagina E.V. Improving cutter performance by the application of nanostructural coatings. *Russian Engineering Research*, 2010, vol. 30, no. 3, pp. 235–242. EDN: [NBGWUR](#).
3. Li Mingxing, Fan Zhiyu, Zhang Wenhai, Zhang Jiankang. Mechanics and Cutting Performance of Multilayer Nanostructured TiAlN/TiSiN/ZrN Coatings. *Coatings*, 2024, vol. 14, no. 10, article number 1255. DOI: [10.3390/coatings14101255](#).
4. Liu Jie, Mei Haijuan, Hua Junfang, Wang Juan, Wang Yongchao, Yi Genmiao, Deng Xin. High-Temperature Oxidation and Wear Resistance of TiAlSiN/AlCrN Multilayer Coatings Prepared by Multi-Arc Ion Plating. *Nanomaterials*, 2025, vol. 15, no. 7, article number 503. DOI: [10.3390/nano15070503](#).
5. Belov D.S., Demirov A.P., Blinkov I.V., Sergevnik V.S., Chernogor A.V., Kiryukhantsev-Korneev P.V., Anikin V.N. Structure and properties features of CA-PVD Ti-Al-Ni-N coatings deposited on carbide alloys and tool steel substrates. *Surface and Coatings Technology*, 2024, vol. 494, part I, article number 131348. DOI: [10.1016/j.surfcoat.2024.131348](#).
6. Belov D.S., Klauch D.N., Blinkov I.V., Laptev A.I., Demirov A.P. Durability of cutting tools with deposited ceramic-metal coatings (Ti, Al)N–Cu and (Ti, Al)N–Ni during turning and milling of steels. *Inorganic Materials: Applied Research*, 2024, vol. 15, no. 3, pp. 752–759. DOI: [10.30791/0015-3214-2023-5-37-46](#).
7. Yi Jiyong, Xu Yinchao, Liu Zhixiong, Xiao Lijuan. Effect of TiC Content and TaC Addition in Substrates on Properties and Wear Behavior of TiAlN-Coated Tools. *Coatings*, 2022, vol. 12, no. 12, article number 1911. DOI: [10.3390/coatings12121911](#).
8. Jiang Aisheng, Zhao Jinfu, Cui Pengcheng, Liu Zhanqiang, Wang Bing. Effects of TiAlN Coating Thickness on Machined Surface Roughness, Surface Residual Stresses, and Fatigue Life in Turning Inconel 718. *Metals*, 2024, vol. 14, no. 8, article number 940. DOI: [10.3390/met14080940](#).
9. Kovalev A.I., Vakhrushev V.O., Konovalov E.P., Fox-Rabinovich G.S., Wainstein D.L., Dmitrievskii S.A., Mukhsinova A.D. Features of the Oxidation of Multilayer (TiAlCrSiY)N/(TiAlCr)N Nanolaminated PVD Coating during Temperature Annealing. *Coatings*, 2023, vol. 13, no. 2, article number 287. DOI: [10.3390/coatings13020287](#).
10. Ly Chang Trung, Tran Thien Phuc. Wear Mechanism of an AlCrN-Coated Solid Carbide Endmill Cutter and Machined Surface Quality under Eco-Friendly Settings during Open Slot Milling of Tempered JIS SKD11 Steel. *Coatings*, 2024, vol. 14, no. 8, article number 923. DOI: [10.3390/coatings14080923](#).
11. Sebbe N.P.V., Fernandes F., Silva F.J.G., Pedrosa A.F.V., Sales-Contini R.C.M., Barbosa M.L.S., Durao L.M., Magalhaes L.L. Wear Behavior of TiAlVN-Coated Tools in Milling Operations of INCONEL® 718. *Coatings*, 2024, vol. 14, no. 3, article number 311. DOI: [10.3390/coatings14030311](#).
12. Vereschaka A., Milovich F., Andreev N., Migranov M., Alexandrov I., Muranov A., Mikhailov M., Tatarkanov A. Influence of Cutting Speed during the Turning of Inconel 718 on Oxidation Wear Pattern on the Zr-ZrN-(Zr,Mo,Al)N Composite Nanostructured Coating. *Journal of Composites Science*, 2023, vol. 7, no. 1, article number 18. DOI: [10.3390/jcs7010018](#).
13. Grigoriev S., Vereschaka A., Uglov V., Milovich F., Cherenda M., Andreev N., Migranov M., Seleznev A. Influence of tribological properties of Zr-ZrN-(Zr,Cr,Al)N and Zr-ZrN-(Zr,Mo,Al)N multilayer nanostructured coatings on the cutting properties of coated tools during dry turning of Inconel 718 alloy. *Wear*, 2023, vol. 512-513, article number 204521. DOI: [10.1016/j.wear.2022.204521](#).
14. Grigoriev S., Vereschaka A., Milovich F., Tabakov V., Sitnikov N., Andreev N., Bublikov J., Sotova C. Investigation of the properties of Ti-TiN-(Ti,Al,Nb,Zr)N composite coating and its efficiency in increasing wear resistance of metal cutting tools. *Surface and Coatings Technology*, 2021, vol. 421, article number 127432. DOI: [10.1016/j.surfcoat.2021.127432](#).
15. Sousa V.F.C., Fernandes F., Silva F.J.G., Costa R.D.F.S., Sebbe N., Sales-Contini R.C.M. Wear Behavior Phenomena of TiN/TiAlN HiPIMS PVD-Coated Tools on Milling Inconel 718. *Metals*, 2023, vol. 13, no. 4, article number 684. DOI: [10.3390/met13040684](#).
16. Wang Rui, Yang Dayong, Wang Wei, Wei Furu, Lu Yuwei, Li Yuqi. Tool Wear in Nickel-Based Superalloy Machining: An Overview. *Processes*, 2022, vol. 10, no. 11, article number 2380. DOI: [10.3390/pr10112380](#).
17. Ly Chanh Trung, Tran Thien Phuc. Performance of TiSiN/TiAlN-Coated Carbide Tools in Slot Milling of Hastelloy C276 with Various Cooling Strategies. *Lubricants*, 2025, vol. 13, no. 7, article number 316. DOI: [10.3390/lubricants13070316](#).
18. Freitas F.R.S., Casais R.C.B., Silva F.J.G., Sebbe N.P.V., Martinho R.P., Sousa V.F.C., Sales-Contini R.C.M., Fernandes F. Wear Behavior of TiAlN/DLC Coating on Tools in Milling Copper–Beryllium Alloy AMPCOLOY® 83. *Coatings*, 2024, vol. 14, no. 11, article number 1354. DOI: [10.3390/coatings14111354](#).
19. Tabakov V.P., Chikhranov A.V. Determination of the mechanical characteristics of wear-resistant ion-plasma coatings based on titanium nitride. *Izvestia of Samara Scientific Center of the Russian Academy of Sciences*, 2010, vol. 12, no. 4, pp. 292–297. EDN: [MSPSYH](#).
20. Tabakov V.P., Smirnov M.Yu., Tsirkin A.V., Chikhranov A.V. Fracture strength of two-element nitride ion-plasmous coatings. *Uprochnyayushchie tekhnologii i pokrytiya*, 2007, no. 12, pp. 15–19. EDN: [IJCJFV](#).

СПИСОК ЛИТЕРАТУРЫ

1. Zhou Jun, Liao Hengcheng, Chen Hongmei, Feng Di, Zhu Weijun. Realizing strength-ductility combination of Fe_{3.5}Ni_{3.5}Cr₂MnAl_{0.7} high-entropy alloy via coherent dual-phase structure // *Vacuum*. 2023. Vol. 215. Article number 112297. DOI: [10.1016/j.vacuum.2023.112297](#).
2. Кабалдин Ю.Г., Серый С.В., Муравьев С.Н., Просолович А.А., Симагина Е.В. Повышение работоспособности режущего инструмента осаждением наноструктурных покрытий // *Вестник Машиностроения*. 2010. № 3. С. 41–49. EDN: [NBGWUR](#).
3. Li Mingxing, Fan Zhiyu, Zhang Wenhai, Zhang Jiankang. Mechanics and Cutting Performance of Multilayer Nanostructured TiAlN/TiSiN/ZrN Coatings // *Coatings*.

2024. Vol. 14. № 10. Article number 1255. DOI: [10.3390/coatings14101255](https://doi.org/10.3390/coatings14101255).
4. Liu Jie, Mei Haijuan, Hua Junfang, Wang Juan, Wang Yongchao, Yi Genmiao, Deng Xin. High-Temperature Oxidation and Wear Resistance of TiAlSiN/AlCrN Multilayer Coatings Prepared by Multi-Arc Ion Plating // *Nanomaterials*. 2025. Vol. 15. № 7. Article number 503. DOI: [10.3390/nano15070503](https://doi.org/10.3390/nano15070503).
 5. Belov D.S., Demirov A.P., Blinkov I.V., Sergevnin V.S., Chernogor A.V., Kiryukhantsev-Korneev P.V., Anikin V.N. Structure and properties features of CA-PVD Ti-Al-Ni-N coatings deposited on carbide alloys and tool steel substrates // *Surface and Coatings Technology*. 2024. Vol. 494. Part I. Article number 131348. DOI: [10.1016/j.surfcoat.2024.131348](https://doi.org/10.1016/j.surfcoat.2024.131348).
 6. Белов Д.С., Клауч Д.Н., Блинокв И.В., Лаптев А.И., Демиров А.П. Стойкость режущего инструмента с осажденными керамико-металлическими покрытиями (Ti,Al)N - Cu и (Ti,Al)N - Ni при точении и фрезеровании сталей // *Физика и химия обработки материалов*. 2023. № 5. С. 37–46. DOI: [10.30791/0015-3214-2023-5-37-46](https://doi.org/10.30791/0015-3214-2023-5-37-46).
 7. Yi Jiyong, Xu Yinchao, Liu Zhixiong, Xiao Lijuan. Effect of TiC Content and TaC Addition in Substrates on Properties and Wear Behavior of TiAlN-Coated Tools // *Coatings*. 2022. Vol. 12. № 12. Article number 1911. DOI: [10.3390/coatings12121911](https://doi.org/10.3390/coatings12121911).
 8. Jiang Aisheng, Zhao Jinfu, Cui Pengcheng, Liu Zhanqiang, Wang Bing. Effects of TiAlN Coating Thickness on Machined Surface Roughness, Surface Residual Stresses, and Fatigue Life in Turning Inconel 718 // *Metals*. 2024. Vol. 14. № 8. Article number 940. DOI: [10.3390/met14080940](https://doi.org/10.3390/met14080940).
 9. Kovalev A.I., Vakhrushev V.O., Konovalov E.P., Fox-Rabinovich G.S., Wainstein D.L., Dmitrievskii S.A., Mukhsinova A.D. Features of the Oxidation of Multilayer (TiAlCrSiY)N/(TiAlCr)N Nanolaminated PVD Coating during Temperature Annealing // *Coatings*. 2023. Vol. 13. № 2. Article number 287. DOI: [10.3390/coatings13020287](https://doi.org/10.3390/coatings13020287).
 10. Ly Chang Trung, Tran Thien Phuc. Wear Mechanism of an AlCrN-Coated Solid Carbide Endmill Cutter and Machined Surface Quality under Eco-Friendly Settings during Open Slot Milling of Tempered JIS SKD11 Steel // *Coatings*. 2024. Vol. 14. № 8. Article number 923. DOI: [10.3390/coatings14080923](https://doi.org/10.3390/coatings14080923).
 11. Sebbe N.P.V., Fernandes F., Silva F.J.G., Pedroso A.F.V., Sales-Contini R.C.M., Barbosa M.L.S., Duraõ L.M., Magalhaes L.L. Wear Behavior of TiAlVN-Coated Tools in Milling Operations of INCONEL® 718 // *Coatings*. 2024. Vol. 14. № 3. Article number 311. DOI: [10.3390/coatings14030311](https://doi.org/10.3390/coatings14030311).
 12. Vereschaka A., Milovich F., Andreev N., Migranov M., Alexandrov I., Muranov A., Mikhailov M., Tatarkanov A. Influence of Cutting Speed during the Turning of Inconel 718 on Oxidation Wear Pattern on the Zr-ZrN-(Zr,Mo,Al)N Composite Nanostructured Coating // *Journal of Composites Science*. 2023. Vol. 7. № 1. Article number 18. DOI: [10.3390/jcs7010018](https://doi.org/10.3390/jcs7010018).
 13. Grigoriev S., Vereschaka A., Uglov V., Milovich F., Cherenda M., Andreev N., Migranov M., Seleznev A. Influence of tribological properties of Zr-ZrN-(Zr,Cr,Al)N and Zr-ZrN-(Zr,Mo,Al)N multilayer nanostructured coatings on the cutting properties of coated tools during dry turning of Inconel 718 alloy // *Wear*. 2023. Vol. 512-513. Article number 204521. DOI: [10.1016/j.wear.2022.204521](https://doi.org/10.1016/j.wear.2022.204521).
 14. Grigoriev S., Vereschaka A., Milovich F., Tabakov V., Sitnikov N., Andreev N., Bublikov J., Sotova C. Investigation of the properties of Ti-TiN-(Ti,Al,Nb,Zr)N composite coating and its efficiency in increasing wear resistance of metal cutting tools // *Surface and Coatings Technology*. 2021. Vol. 421. Article number 127432. DOI: [10.1016/j.surfcoat.2021.127432](https://doi.org/10.1016/j.surfcoat.2021.127432).
 15. Sousa V.F.C., Fernandes F., Silva F.J.G., Costa R.D.F.S., Sebbe N., Sales-Contini R.C.M. Wear Behavior Phenomena of TiN/TiAlN HiPIMS PVD-Coated Tools on Milling Inconel 718 // *Metals*. 2023. Vol. 13. № 4. Article number 684. DOI: [10.3390/met13040684](https://doi.org/10.3390/met13040684).
 16. Wang Rui, Yang Dayong, Wang Wei, Wei Furui, Lu Yuwei, Li Yuqi. Tool Wear in Nickel-Based Superalloy Machining: An Overview // *Processes*. 2022. Vol. 10. № 11. Article number 2380. DOI: [10.3390/pr10112380](https://doi.org/10.3390/pr10112380).
 17. Ly Chanh Trung, Tran Thien Phuc. Performance of Ti-SiN/TiAlN-Coated Carbide Tools in Slot Milling of Hastelloy C276 with Various Cooling Strategies // *Lubricants*. 2025. Vol. 13. № 7. Article number 316. DOI: [10.3390/lubricants13070316](https://doi.org/10.3390/lubricants13070316).
 18. Freitas F.R.S., Casais R.C.B., Silva F.J.G., Sebbe N.P.V., Martinho R.P., Sousa V.F.C., Sales-Contini R.C.M., Fernandes F. Wear Behavior of TiAlN/DLC Coating on Tools in Milling Copper-Beryllium Alloy AMPICOLOY® 83 // *Coatings*. 2024. Vol. 14. № 11. Article number 1354. DOI: [10.3390/coatings14111354](https://doi.org/10.3390/coatings14111354).
 19. Табаков В.П., Чихранов А.В. Определение механических характеристик износостойких ионно-плазменных покрытий на основе нитрида титана // *Известия Самарского научного центра Российской академии наук*. 2010. Т. 12. № 4. С. 292–297. EDN: [MSPSYH](https://www.edn.ru/MSPSYH).
 20. Табаков В.П., Смирнов М.Ю., Циркин А.В., Чихранов А.В. Трещиностойкость двухэлементных нитридных ионно-плазменных покрытий // *Упрочняющие технологии и покрытия*. 2007. № 12. С. 15–19. EDN: [IJCJFV](https://www.edn.ru/IJCJFV).

УДК 621.9.025

doi: <https://doi.org/10.18323/2782-4039-2025-4-74-8>

Влияние условий обработки на изнашивание контактных площадок и работоспособность твердосплавного инструмента с износостойкими покрытиями

ТабакOV Владимир Петрович^{1,4}, доктор технических наук, профессор

Морозов Олег Игоревич*^{1,2,5}, кандидат технических наук, доцент

Каменов Ренат Уахитович^{2,3,6}, кандидат технических наук

¹Ульяновский государственный технический университет, Ульяновск (Россия)

²Национальный исследовательский университет «Московский институт электронной техники», Москва (Россия)

³Тольяттинский государственный университет, Тольятти (Россия)

*E-mail: oi.morozov@ulstu.ru

⁴ORCID: <https://orcid.org/0000-0002-2568-9401>

⁵ORCID: <https://orcid.org/0000-0001-8241-2591>

⁶ORCID: <https://orcid.org/0000-0001-9181-5704>

Поступила в редакцию 28.08.2025

Пересмотрена 06.10.2025

Принята к публикации 10.11.2025

Аннотация: Использование износостойких покрытий на контактных площадках инструмента является одним из наиболее эффективных способов повышения его долговечности и стабильности работы. Однако при обработке труднообрабатываемых материалов эффективность таких покрытий заметно снижается, что делает актуальными задачи получения новых данных о механизме их разрушения и разработки более совершенных составов. В работе исследовано влияние условий обработки, свойств обрабатываемого материала и состава износостойких покрытий на изнашивание контактных площадок и работоспособность твердосплавного инструмента. Рассматривались однослойные покрытия TiN, TiZrN и TiSiN; проведена оценка их напряженного состояния и циклической трещиностойкости. Изучение контактных площадок твердосплавных пластин выполнялось с использованием оптических методов, а испытания на износ – при токарной обработке на специализированном оборудовании. Показано, что как тип обрабатываемого материала, так и режимы резания существенно влияют на характер разрушения покрытия и период стойкости инструмента. Установлено преимущество двухэлементных покрытий, обладающих повышенными механическими характеристиками и выраженными сжимающими остаточными напряжениями, что способствует росту циклической трещиностойкости и повышает сопротивляемость разрушению. Полученные результаты могут быть использованы при разработке технологических процессов финишной обработки труднообрабатываемых материалов, особенно в условиях минимального применения смазочно-охлаждающих жидкостей (MQL) или полного отказа от смазочно-охлаждающих технологических сред.

Ключевые слова: износостойкое покрытие; твердосплавный инструмент; трещиностойкость; изнашивание; работоспособность; труднообрабатываемые материалы

Благодарности: Исследование выполнено за счет гранта Российского научного фонда № 22-19-00298-П, <https://rscf.ru/project/22-19-00298/>.

Для цитирования: Табаков В.П., Морозов О.И., Каменов Р.У. Влияние условий обработки на изнашивание контактных площадок и работоспособность твердосплавного инструмента с износостойкими покрытиями // Frontier Materials & Technologies. 2025. № 4. С. 89–101. DOI: <https://doi.org/10.18323/2782-4039-2025-4-74-8>.